# The ATP-dependent chromatin remodeling enzyme CHD7 regulates pro-neural gene expression and neurogenesis in the inner ear

**Elizabeth A. Hurd[1], Heather K. Poucher[1], Katherine Cheng[1], Yehoash Raphael[2] and Donna M. Martin[1,3,*]**

## SUMMARY

Inner ear neurogenesis is positively regulated by the pro-neural bHLH transcription factors *Ngn1* and *NeuroD*, but the factors that act upstream of this regulation are not well understood. Recent evidence in mouse and *Drosophila* suggests that neural development depends on proper chromatin remodeling, both for maintenance of neural stem cells and for proper neuronal differentiation. Here, we show that CHD7, an ATP-dependent chromatin remodeling enzyme mutated in human CHARGE syndrome, is necessary for proliferation of inner ear neuroblasts and inner ear morphogenesis. Conditional deletion of *Chd7* in the developing otocyst using *Foxg1-Cre* resulted in cochlear hypoplasia and complete absence of the semicircular canals and cristae. Conditional knockout and null otocysts also had reductions in vestibulo-cochlear ganglion size and neuron number in combination with reduced expression of *Ngn1, Otx2* and *Fgf10*, concurrent with expansion of the neural fate suppressor *Tbx1* and reduced cellular proliferation. Heterozygosity for *Chd7* mutations had no major effects on expression of otic patterning genes or on cell survival, but resulted in decreased proliferation within the neurogenic domain. These data indicate that epigenetic regulation of gene expression by CHD7 must be tightly coordinated for proper development of inner ear neuroblasts.

KEY WORDS: *Chd7*, Chromatin remodeling, Gene regulation, CHARGE syndrome, Neural development, Mouse

## INTRODUCTION

The vertebrate inner ear is a complex organ that is necessary for transducing hearing and balance signals. In mammals, the inner ear develops from the otic placode, an ectodermal thickening that is adjacent to the hindbrain that gives rise to the otocyst (Alsina et al., 2009; Bok et al., 2007). Axial specification of the otocyst, defined by regionalization of gene expression, is essential for generation of neuroblasts and normal development of inner ear structures (Alsina et al., 2009; Bok et al., 2007; Fekete and Wu, 2002). One of the earliest cell fate decisions during inner ear development is neural competence (Fekete and Wu, 2002). This event is concurrent with otic placode formation, and is defined by expression of the basic helix-loop-helix protein neurogenin 1 (Ngn1) (Alsina et al., 2009). *Ngn1*-null mice fail to express neural fate markers such as *NeuroD* (*Neurod1*), and lack all sensory neurons of the inner ear (Ma et al., 2000; Ma et al., 1998). Expression of *Ngn1* and *NeuroD*, along with lunatic fringe (*Lfng*), *Otx2* and the fibroblast growth factor *Fgf10*, defines the anterior region of the developing otocyst (Alsina et al., 2009; Bok et al., 2007; Fekete and Wu, 2002). Posteriorly expressed genes, such as *Tbx1* (T-box transcription factor 1), stabilize the neurogenic region by inhibiting *Ngn1*, creating the otic anteroposterior axis (for a review, see Bok et al., 2007). The neurogenic region is also restricted ventrally by dorsal *Wnt* signaling from the neural tube and ventral *Sonic hedgehog* (*Shh*) signaling from the notochord and floor plate of the hindbrain (Riccomagno et al., 2002; Riccomagno et al., 2005).

After acquisition of neural competence and expression of pro-neural genes, cells within the anteroventral region of the otocyst delaminate and proliferate to form neurons of the statoacoustic (future vestibulo-cochlear) ganglion (Fritzsch et al., 2006; Fritzsch et al., 1999; Sanchez-Calderon et al., 2007). After delamination, ganglionic neuroblasts continue to proliferate and later differentiate into bipolar neurons that send projections to the brain and to inner ear sensory end organs (Fritzsch et al., 2005). As bipolar neurons develop, pro-neural fate markers are downregulated and genes that are essential for neuronal survival and extension, including *TrkB* and *TrkC* neurotrophin receptors, are expressed (Pirvola and Ylikoski, 2003; Sanchez-Calderon et al., 2007). Non-ganglionic progenitors in the neurogenic region of the otic epithelium are fated to develop into cells that occupy the sensory epithelium of the vestibular maculae (Raft et al., 2007).

Haploinsufficiency for CHD7, the chromatin remodeling enzyme mutated in CHARGE syndrome (Vissers et al., 2004), results in severe malformations of the lateral and posterior semicircular canals in both humans and mice (Adams et al., 2007; Bosman et al., 2005; Hurd et al., 2007). Adult *Chd7[Gt/+]* mutant mice also have defects in innervation to the adult posterior crista within the ear (Adams et al., 2007), and reduced neural stem cell proliferation in the olfactory epithelium (Layman et al., 2009). CHD7 belongs to a family of nine mammalian CHD proteins characterized by the presence of two chromodomains N-terminal to an SNF2 ATP-dependent helicase domain (Woodage et al., 1997). CHD proteins are proposed to repress or activate downstream target genes, via participation in chromatin remodeling complexes that have epigenetic functions in proliferation (Rodriguez-Paredes et al., 2009) and cell fate (Takada et al., 2007).

[1]Department of Pediatrics, The University of Michigan, Ann Arbor, MI 48109, USA. [2]Department of Otolaryngology, The University of Michigan, Ann Arbor, MI 48109, USA. [3]Department of Human Genetics, The University of Michigan, Ann Arbor, MI 48109, USA.

*Author for correspondence (donnamm@umich.edu)

Downstream targets have been identified for some CHD proteins in cultured cells (Nioi et al., 2005; Tai et al., 2003; Tong et al., 1998; Vertegaal et al., 2006), and recent research in *Xenopus* has shown that CHD7 associates with the PBAF (polybromo- and BRG1-associated factor-containing) complex to promote neural crest gene expression and cell migration (Bajpai et al., 2010). In vitro chromatin immunoprecipitation followed by microarray analysis (ChIP-chip) has also shown that CHD7 binds to sites of methylated histones (H3K4me) that are associated with sites of active transcription (Schnetz et al., 2009). CHD7 is thought to directly enhance transcription by chromodomain binding to H3K4me, which regulates access to DNA for other transcriptional activators via the ATP-dependent helicase domain (Schnetz et al., 2009). CHD7 is predicted to bind to thousands of sites throughout the mammalian genome, including transcription start sites and enhancer regions (Schnetz et al., 2009). Comparisons of CHD7 targets between different cell lines, along with the variable penetrance of CHARGE phenotypes, suggest that CHD7-binding specificity and target gene expression are likely to be tissue and developmental stage specific. In this study, we report the generation of the first *Chd7^flox* allele and its use in investigating the effect of otocyst-specific CHD7 deletion.

## MATERIALS AND METHODS

### Generation of the *Chd7^flox* allele

A BAC clone containing *Chd7* genomic sequences (RP23-121H12) was obtained from Children's Hospital Oakland Research Institute (Oakland, CA). Regions of homology were engineered as shown in Fig. 1. The linearized targeting vector was electroporated into W4 (129S6/SvEvTac) ES cells and selected for by neomycin resistance. Positive clones were identified by PCR and confirmed using Southern blot analysis. Targeted clones were injected into C57BL/6 blastocysts and founder males (*Chd7^floxfrtneokan/+*) bred with C57BL/6 females. Resulting F1 progeny were genotyped as shown in Fig. 1. *Chd7^floxfrtneokan/+* female mice were bred with FLPeR male mice (Jackson Laboratory #003496) to remove the neo/kan cassette to generate *Chd7^+/flox* mice.

### Mice

*Chd7^Gt/+* mice were generated as previously described (Hurd et al., 2007). Mice were maintained by backcrossing with 129S1/Sv1mJ (Jackson Laboratory) mice to generation N5-N7 or B6D$_2$F$_1$/J (Jackson Laboratory #100006) mice to N2-N3. *Chd7^flox/+* mice were mated with *Foxg1-Cre* or *EIIa-Cre* mice. *Foxg1-Cre* mice were maintained on the Swiss Webster (Charles River Laboratories #F44281) background and genotyped for *Cre* as described (Hebert and McConnell, 2000).

### Whole-mount β-galactosidase labeling

Postnatal day 0 (P0) pups were euthanized and temporal bones dissected. The oval and round windows and apex of the cochlea were perforated, fixed in 2% paraformaldehyde for 1 hour at room temperature, and washed in PBS followed by X-gal wash buffer [sodium phosphate buffer (pH 7.4) with 2 mM MgCl$_2$ and 0.02% NP-40 (Sigma, St Louis, MO)]. Ears were stained in X-gal wash buffer containing 0.02 mg/ml X-gal (Roche, Indianapolis, IN), 5 mM potassium ferrocyanide (Fisher, Pittsburgh, PA), 5 mM potassium ferricyanide (Fisher), and 0.33% *N-N*-dimethylformamide (Sigma), post-fixed in 4% paraformaldehyde and cleared using a glycerol gradient.

### Immunofluorescence

Timed pregnancies were established and the morning of plug identification designated as E0.5. Embryos were harvested and amniotic sacs collected for PCR genotyping as described (Hurd et al., 2007). Embryos were fixed in 4% paraformaldehyde for 30 minutes (E9.5-E10.5) to 1.5 hours (E11.5-E12.5), then washed in PBS and dehydrated in ethanol. Embryos were embedded in paraffin and sectioned at 7 µm or incubated in 30% sucrose for frozen sectioning at 12 µm as described previously (Martin et al., 2004).

For each antibody, multiple sections from at least four ears of each genotype were tested. The following antibodies were incubated at 4°C overnight: polyclonal rabbit anti-CHD7 antibody (1:1000, Abcam, Cambridge, MA); mouse anti-β-tubulin III (1:1500, TuJ1; Covance, Richmond, CA); rabbit anti-NeuroD (1:600, gift of Jacques Drouin); mouse anti-Islet1 (1:500, Developmental Studies Hybridoma Bank, Iowa City, IA); and rabbit anti-TBX1 (1:1000, gift of Bernice Morrow). Direct secondary antibodies conjugated to Alexa488 and Alexa555 were purchased from Invitrogen. Alternatively, secondary detection was performed using biotinylated antibodies (Vector Laboratories, Burlingame, CA) followed by HRP-streptavidin Tyramide signal amplification (TSA) (Invitrogen).

### Paint filling

Timed pregnancies were established and embryos collected at E14.5, after cervical dislocation and hysterectomy. Embryos were washed briefly in PBS, fixed in Bodian's fixative and cleared in methyl salicylate. Heads were bisected, brains removed and ears were injected with 3% WhiteOut in methylsalicylate, as described previously (Hurd et al., 2007).

### In situ hybridization

In situ hybridization was performed on paraffin embedded embryo sections using digoxigenin-labeled riboprobes as previously described (Martin et al., 2002) at annealing temperatures between 55°C and 65°C. For each probe, multiple sections from at least four ears of each genotype were tested. RNA probes were provided by Doris Wu (*Otx2* and *Lfng*), Deneen Wellik (*Eya1*) and Brigid Hogan (*Fgf10*).

### Cell proliferation and cell death assays

Wild-type and *Chd7^Gt/+* E9.5-E10.5 embryos were processed as above for immunofluorescence. For cell proliferation assays, serial adjacent sections were labeled with rabbit anti-phosphohistone H3 (1:200, Millipore, Billerica, MA) followed by incubation with anti-rabbit AlexaFluor488-conjugated secondary antibody (Invitrogen) and co-stained with DAPI (1:50, Invitrogen). Cell death assays were performed on serial adjacent sections using Fluorescein-FragEL DNA fragmentation detection kit (Calbiochem, San Diego, CA) according to the manufacturer's instructions.

### Statistical analyses

Cell counts were performed on at least four embryos (eight ears) of each genotype at each time point. One-way ANOVA with Tukey's post-hoc analysis was performed when comparing groups of three genotypes or more. Student's *t*-tests with Welch's correction were performed to determine statistical significance of H3-positive cells in the neurogenic region. Standard error of the mean (s.e.m.) was calculated for each value.

## RESULTS

### Generation of a conditional *Chd7* null allele

We have previously reported the generation of a *Chd7* genetrap (*Chd7^Gt*) allele in which Rosafary genetrap sequences are inserted in non-coding sequences upstream of the ATG-containing exon 2 (Hurd et al., 2007). Homozygous *Chd7*-null mice (*Chd7^Gt/Gt*) are lethal after E10.5, prohibiting examination of *Chd7*-null inner ears beyond the otocyst stage (Hurd et al., 2007). Thus, we generated a conditional *Chd7^floxfrtneokan* allele for use in tissue-specific deletions (Fig. 1A). We confirmed the generation of a conditional *Chd7*-null allele by crossing *Chd7^+/flox* mice with a ubiquitous *Cre*-expressing recombinase, *EIIA-Cre*, generating *Chd7^+/−* mice (Fig. 1). *Chd7^+/−* mice displayed circling and head-bobbing behaviors, and lateral semicircular canal abnormalities similar to those observed in *Chd7^Gt/+* mice (data not shown). CHD7 immunofluorescence was present in E10.5 *Chd7^+/−* embryos and absent in *Chd7^−/−* embryos (Fig. 1D). Thus, *Chd7^+/−* mice have similar phenotypes to *Chd7^Gt/+* mice, and the *Chd7^flox* allele can be used for conditional *Chd7* mutagenesis.
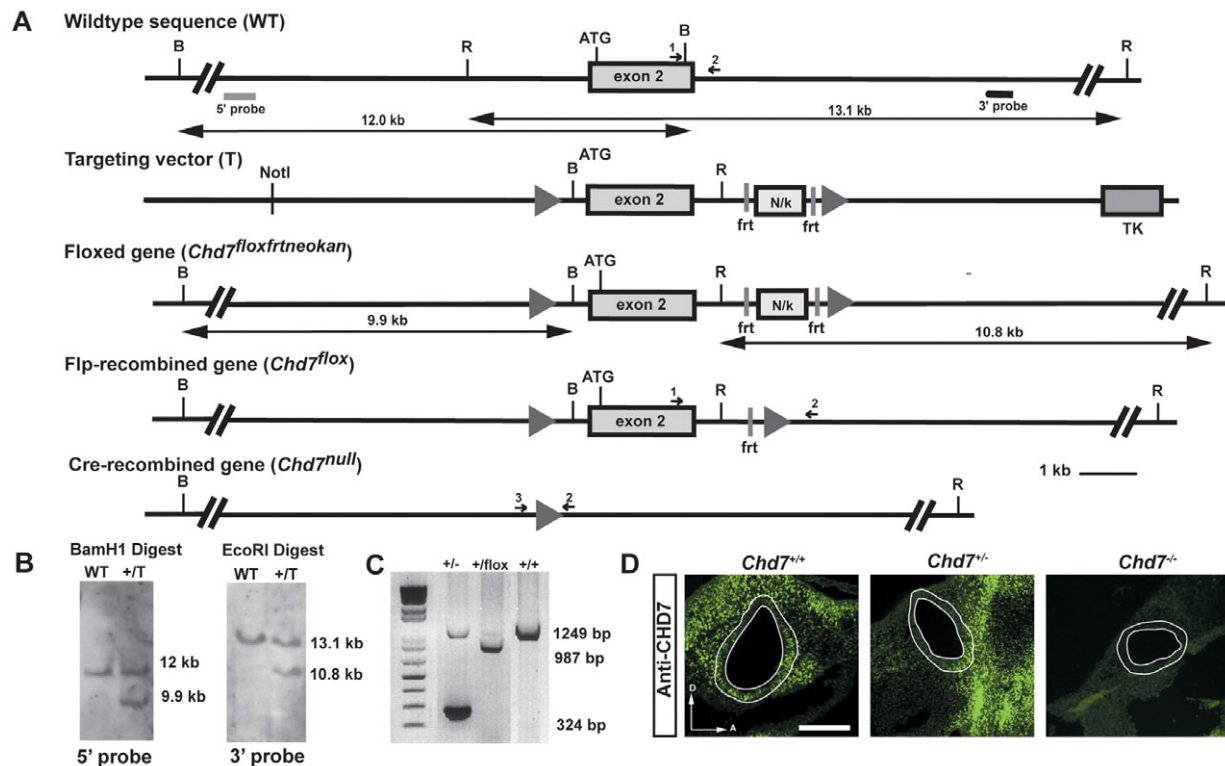
**Fig. 1. Generation of a conditional *Chd7* allele.** (**A**) Recombineering techniques were used to introduce a neomycin/kanamycin (N/k) cassette downstream of *Chd7* exon 2. LoxP sites (grey arrowheads) were positioned 5' of exon 2 and 3'of the N/k cassette. (**B**) Targeted ES cells were confirmed by Southern blotting, using probes indicated in A. Genomic DNA was digested with *Eco*RI (R) producing either a 12 kb wild-type (WT) or 9.9 kb targeted (T) product, whereas digestion with *Bam*HI (B) and screening with a 3' probe detected either a 13.1 kb (WT) or 10.8 kb targeted (T) product. (**C**) PCR genotyping of DNA from *Ella-Cre;Chd7$^{+/flox}$* mice. Bands of 1249, 987 and 324 bp represent *Chd7$^{+}$*, *Chd7$^{flox}$* and *Chd7$^{-}$* alleles, respectively. (**D**) CHD7 immunofluorescence on E10.5 sagittal frozen sections. *Chd7$^{+/-}$* embryos have reduced *Chd7* expression compared with *Chd7$^{+/+}$*, whereas CHD7 protein is absent in *Chd7$^{-/-}$* embryos. White lines in D represent the outline of the otic epithelium. Scale bar: 100 μm.

## *Chd7* conditional null mice display severe inner ear abnormalities

To generate mice with inner ear-specific *Chd7* deficiency, we used *Foxg1-Cre* mice that express *Cre* recombinase in the otic vesicle by E8.5 (Hebert and McConnell, 2000). We mated *Chd7$^{Gt/+}$* mice, which express β-galactosidase, with *Foxg1-Cre* mice to generate *Foxg1-Cre;Chd7$^{Gt/+}$* males. *Foxg1-Cre;Chd7$^{Gt/+}$* males were then crossed with *Chd7$^{flox/flox}$* females for embryo collection. This breeding scheme required *Cre* recombination at only one *Chd7* allele and enabled use of β-galactosidase as a reporter of *Chd7*-expressing cells (Fig. 2A). This mating also allowed us to analyze *Foxg1-Cre;Chd7$^{+/flox}$* (conditional heterozygous) phenotypes as important controls for possible *Foxg1* heterozygous effects (Hebert and McConnell, 2000).
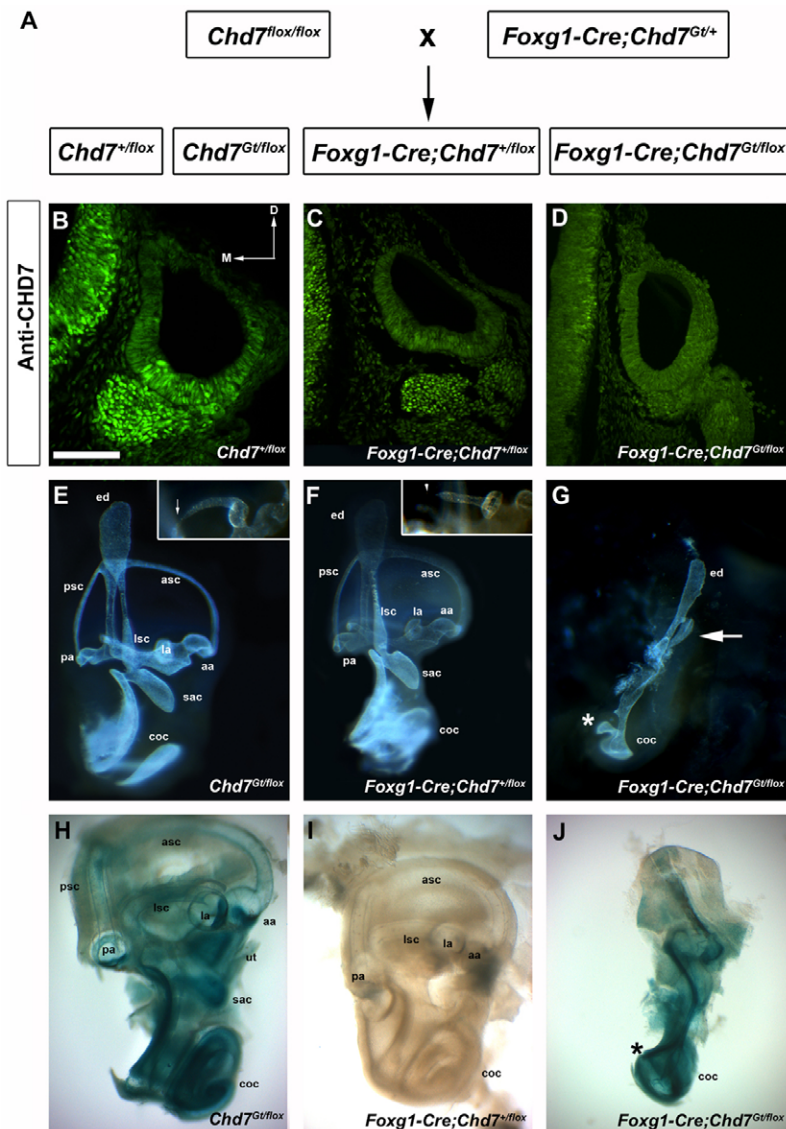
*Foxg1-Cre;Chd7$^{Gt/flox}$* (conditional null) mice displayed medially displaced eyes and shortened snouts compared with control littermates (see Fig. S1 in the supplementary material). Conditional null mice survived only until postnatal day 1, with no obvious milk in the stomach, suggesting early postnatal mortality due to inability to feed. We performed CHD7 immunofluorescence on E10.5 embryos (Fig. 2B-D) to confirm *Cre* recombination. CHD7 immunofluorescence was highest in the anterior ventral region of the E10.5 otocyst in *Chd7$^{+/flox}$* embryos, reduced in conditional heterozygotes, and absent in conditional null embryos (Fig. 2D).

Conditional heterozygous and *Chd7$^{Gt/flox}$* inner ears had defects similar to those previously described in *Chd7$^{Gt/+}$* ears, including truncated or hypoplastic lateral semicircular canals with preserved

anterior semicircular canals, utricles, sacculae and cochleae (Fig. 2E,F) (Hurd et al., 2007). *Chd7$^{Gt/flox}$* inner ears expressed β-galactosidase throughout all six sensory epithelia [maculae of the utricle and saccule; crista ampullaris of the lateral, anterior and posterior canal; and the cochlear epithelium (Fig. 2H)]. By contrast, conditional null inner ears displayed severe structural abnormalities in both vestibular and cochlear structures (Fig. 2G). The conditional null endolymphatic duct and anterior semicircular canal were hypoplastic, whereas the posterior and lateral canals and vestibular sensory organs (cristae, saccule and utricle) were missing (*n*=6) (Fig. 2G). The conditional null cochlea was also severely hypoplastic and undercoiled, with abnormal twisting at the apex. β-Galactosidase staining was observed in the conditional null cochlea and in a dorsal stripe in the vestibule behind the endolymphatic duct (Fig. 2J). The severity of the inner ear phenotype in conditional null inner ears compared with the mild phenotype observed in conditional heterozygous ears also suggests that these defects are not due to double heterozygous mutant effects.

## *Chd7* expression becomes progressively restricted to the vestibulo-cochlear ganglion and sensory tissues

To better understand the defects observed by loss of *Chd7* function within the inner ear, we closely examined CHD7 protein between E9.5-E12.5. CHD7 was widespread in the mesenchyme, otic epithelium and developing vestibulo-cochlear ganglion at E9.5 (see Fig. S2A in the supplementary material). By E10.5, during axial

**Fig. 2. *Foxg1-Cre;Chd7^{Gt/flox}* mice have severe inner ear abnormalities.** (**A**) Breeding scheme used to generate mice with conditional loss of *Chd7* function within the inner ear. (**B-D**) CHD7 is widely expressed in the E10.5 otocyst of *Foxg1-Cre;Chd7^{+/flox}* (B) and *Chd7^{+/flox}* (C) embryos, and is absent from the *Foxg1-Cre;Chd7^{Gt/flox}* otocyst (D). Sections are in the transverse plane, with dorsal towards the top, medial towards the left, and the hindbrain epithelium is on the left, as shown by arrows in B. (**E,F**) *Chd7^{Gt/flox}* and *Foxg1-Cre;Chd7^{+/flox}* E14.5 inner ears have normal anterior and posterior semicircular canals, endolymphatic ducts and cochleae. Inserts in E and F are enlarged images of typical lateral canal defects, including epithelial narrowing (arrow) and truncation (arrowhead). (**G**) *Foxg1-Cre;Chd7^{Gt/flox}* E14.5 ears have no semicircular canals or sensory vestibular structures aside from a rudimentary anterior semicircular canal (arrow) and an undercoiled cochlea with abnormal twisting at the tip of the cochlea (*). The endolymphatic duct (ed) is intact but smaller in *Foxg1-Cre;Chd7^{Gt/flox}* ears. (**H-J**) Staining of P0 inner ears shows strong β-galactosidase expression in *Chd7^{Gt/flox}* vestibular sensory organs [anterior ampulla (aa), lateral ampulla (la), posterior ampulla (pa), saccule (sac) and utricle (ut)] and cochlea (coc). (J) *Foxg1-Cre;Chd7^{Gt/flox}* ears have β-galactosidase staining in the abnormally developed cochlea. Asterisk indicates abnormal twisting at the cochlear tip. Other abbreviations: asc, anterior semicircular canal; lsc, lateral semicircular canal; psc, posterior semicircular canal. Scale bar: 100 μm.

specification, CHD7 was restricted to the anterior and ventral regions of the otocyst (corresponding to the neurogenic domain) and in the developing statoacoustic ganglion (Fig. 2B). At E11.5, CHD7 was highest in the ventral region of the otocyst, which gives rise to the saccule, utricle, cochlea and vestibulo-cochlear ganglion (see Fig. S3B-C in the supplementary material). By E12.5, CHD7 was observed in the vestibulo-cochlear ganglion and cochlea, and at lower levels in the lateral canal primordium (see Fig. S3D-F in the supplementary material). Low levels of CHD7 were also present in the periotic mesenchyme between E10.5 and E12.5 (Fig. 2B and see Fig. S3 in the supplementary material). CHD7 was absent from the endolymphatic duct, consistent with mild ductal hypoplasia in *Chd7* conditional null mice (Fig. 2G). Thus, *Chd7* expression was widespread at the otocyst stage with progressive restriction to the vestibulo-cochlear ganglion and pro-sensory tissues during later inner ear development.

## Expression of *Otx2*, *Fgf10* and *Ngn1* within the otocyst is *Chd7* dependent

Initial patterning of the otocyst dictates later morphogenetic events, including formation of the vestibulo-cochlear ganglion and semicircular canals (Bok et al., 2007). This morphogenetic patterning is established by dynamic gene expression changes that generate unique domains for prospective inner ear structures. We tested whether reduced CHD7 impacts expression of genes implicated in E9.5-E10.5 otocyst patterning. *Otx2*, which regulates cochlear patterning and ganglion development (Miyazaki et al., 2006; Morsli et al., 1999), was retained in E10.5 *Chd7^{Gt/+}* and conditional heterozygotes, but was absent from conditional null and *Chd7^{Gt/Gt}* otocysts (Fig. 3A-E).

*Lfng* expression, which defines a ventral region within the otocyst that gives rise to the saccule and utricle and the organ of Corti, was present in all E9.5-E10.5 *Chd7* mutants, and slightly reduced in the *Chd7^{Gt/Gt}* otocyst (Fig. 3F-J and see Fig. S2B-F in the supplementary material). We also detected normal expression of *Eya1* in E10.5 *Chd7* heterozygotes and conditional null otocysts (Fig. 3K,L,N,O); however, *Eya1* expression was absent from *Chd7^{Gt/Gt}* otocysts (Fig. 3M). The fibroblast growth factor, *Fgf10*, which regulates *Ngn1* expression in the otocyst (Alsina et al., 2004), was reduced in *Chd7^{Gt/+}* and conditional heterozygous embryos and was completely absent from *Chd7^{Gt/Gt}* and conditional null otocysts (Fig. 3P-T). These data suggest that CHD7 is involved in controlling early neurogenic events in the developing ear.
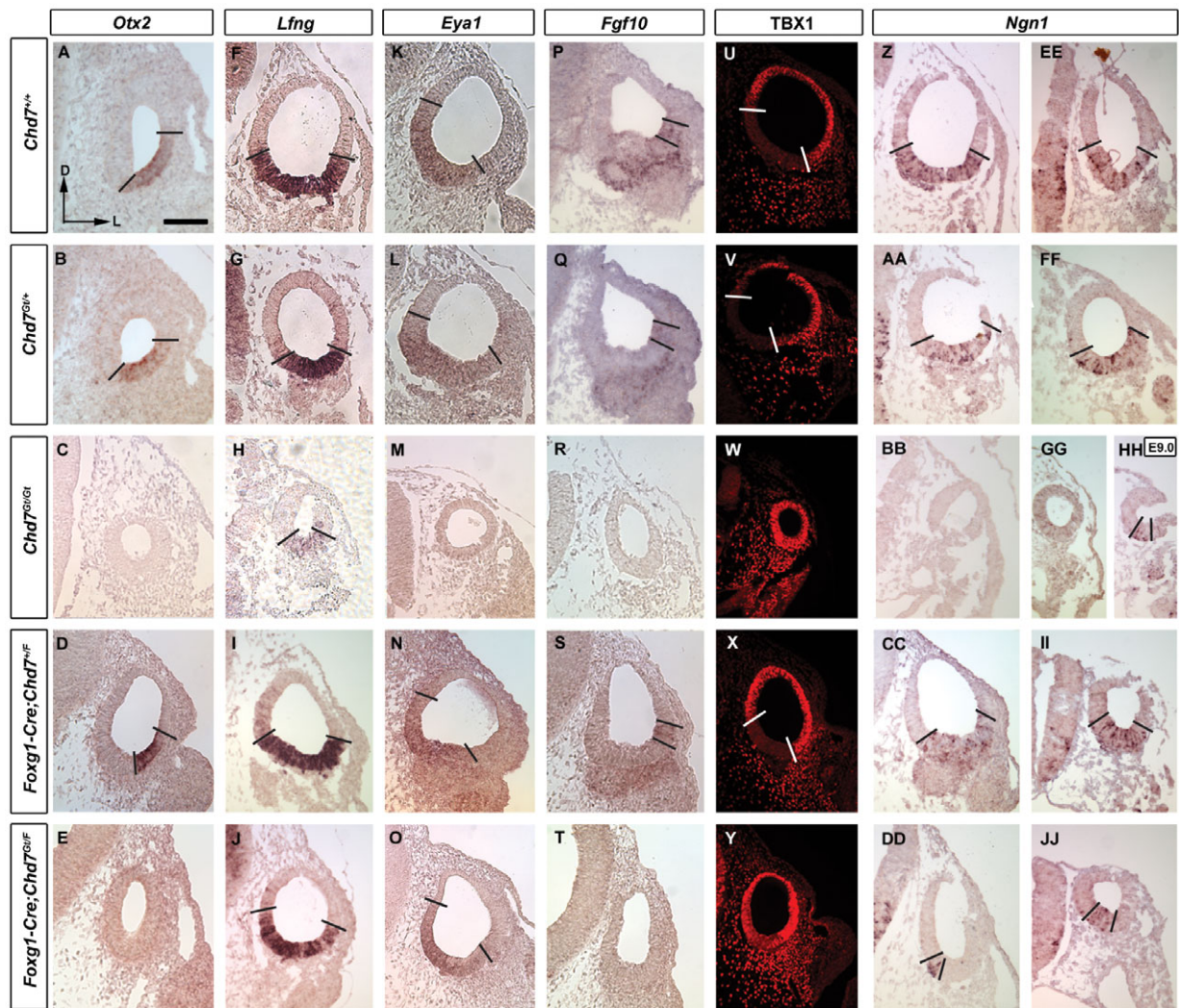
**Fig. 3. Domain-specific patterning in the developing otocyst is sensitive to *Chd7* dose.** All sections are in the transverse plane with dorsal towards the top and lateral towards the right, as shown in A. A-DD are E10.5; EE-GG,II,JJ are E9.5; HH is E9.0. (**A-E**) Expression of the ventral otocyst marker *Otx2* is unchanged in *Chd7^Gt/+* (B) and *Foxg1-Cre;Chd7^+/flox* (D) otocysts compared with wild type, but is absent from *Chd7^Gt/Gt* (C) and *Foxg1-Cre;Chd7^Gt/flox* (E) otocysts. (**F-J**) Ventral *Lfng* expression is conserved in all *Chd7* mutant otocysts, albeit at lower levels in *Chd7^Gt/Gt* (H). (**K-O**) *Eya1* is expressed in *Chd7^Gt/+* (L), *Foxg1-Cre;Chd7^+/flox* (N) and *Foxg1-Cre;Chd7^Gt/flox* (O) otocysts but is absent from *Chd7^Gt/Gt* (M). (**P-T**) *Fgf10* is expressed in *Chd7^Gt/+* (Q) and *Foxg1-Cre;Chd7^+/flox* (S) otocysts, and is absent from *Chd7^Gt/Gt* (R) and *Foxg1-Cre;Chd7^Gt/flox* (T). (**U-Y**) TBX1 protein is expanded ventrally in *Chd7^Gt/Gt* (W) and *Foxg1-Cre;Chd7^Gt/flox* (Y) otocysts compared with wild type (U) and *Chd7^Gt/+* (V). (**Z-JJ**) The *Ngn1* expression domain is maintained in E9.5 and E10.5 *Chd7^Gt/+* (AA,FF) and *Foxg1-Cre;Chd7^+/flox* otocysts (CC,II), is absent from E9.5 and E10.5 *Chd7^Gt/Gt* (BB,GG) and is reduced in *Foxg1-Cre;Chd7^Gt/flox* otocysts (DD,JJ). (HH) *Ngn1* expression is reduced but present in E9.0 *Chd7^Gt/Gt*. Scale bar: 100 μm.

To address whether CHD7 regulates initiation or maintenance of the neurogenic domain, we analyzed expression of the pro-neural marker *Ngn1* in wild-type and *Chd7* mutant tissues. We observed no difference in ventral expression of *Ngn1* between *Chd7* heterozygous mutant and wild-type embryos at E9.5 or E10.5 (Fig. 3Z,AA,EE,FF). However, *Ngn1* expression was absent in E9.5-E10.5 *Chd7^Gt/Gt* embryos (Fig. 3BB,GG) and significantly reduced in E9.5-E10.5 *Chd7* conditional null embryos (Fig. 3DD,JJ). Notably, *Ngn1* expression was present in younger (E9.0) *Chd7^Gt/Gt* otocysts (Fig. 3HH). These observations suggest that CHD7 is required for maintenance, but not necessarily for initiation, of *Ngn1* expression.

Because *Ngn1* expression is inhibited by TBX1 (Raft et al., 2004), we also examined *Chd7* mutants for TBX1 immunofluorescence. Within the dorsal otocyst, TBX1 was maintained in E10.5 *Chd7^Gt/+* embryos but was expanded ventrally in *Chd7^Gt/Gt* and conditional null embryos (Fig. 3U-Y). These results suggest that *Chd7* is important for early otic patterning by positively or negatively regulating expression of genes that promote (*Ngn1*, *Otx2*, *Fgf10*) or inhibit (*Tbx1*) development of the otic neurogenic domain, in a dose-dependent manner.

### *Chd7* is expressed in inner ear neuroblasts and regulates their formation

Vestibulo-cochlear ganglion neurons are formed in the mouse between E9.5 and E14.5, by delamination of ventral otic epithelial neural progenitors into the surrounding mesenchyme (Fritzsch et al., 1999). Delaminated ganglionic neuroblasts express *Ngn1*, *Islet1*, neuron-specific β-Tubulin III, and *NeuroD*, and continue to proliferate prior to aggregation and subsequent formation of

DEVELOPMENT
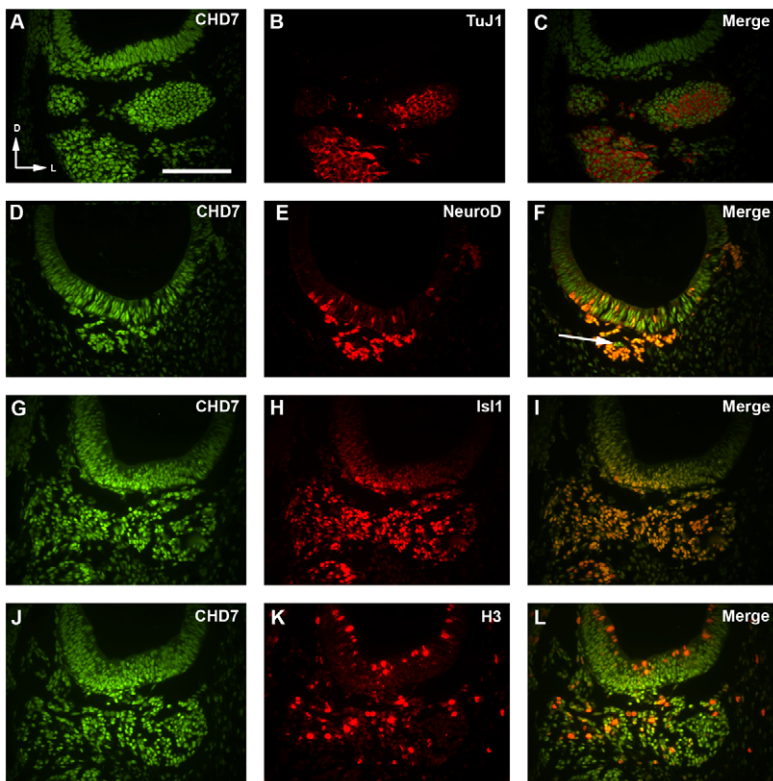
**Fig. 4. CHD7 is concentrated in early inner ear neuroblasts of the vestibulo-cochlear ganglion.** Co-immunofluorescence of anti-CHD7 (**A,D,G,J**), with anti-β-tubulin III (TuJ1) (**B**), NeuroD (**E**) or Islet1 (**H**) shows doubly positive cells throughout the otocyst and ganglia of E10.5 wild-type embryos. (**C,F,I**) Merged images. Mitotic cells within the ventral otocyst and ganglion are also CHD7 positive, as shown by co-localization (**L**) with anti-phosphohistone H3 (**K**). Arrow in F represents CHD7-positive, NeuroD-negative cells. Scale bar: 100 μm.

separate vestibular and cochlear ganglia (Sanchez-Calderon et al., 2007). As *Chd7* is highly expressed in the anterior ventral region of the otocyst and vestibulo-cochlear ganglion, we hypothesized that CHD7 may colocalize with markers of pro-neural genes and have a role in neurogenesis. We observed CHD7 in β-Tubulin III-positive neurons throughout the E10.5 vestibulo-cochlear ganglion (Fig. 4A-C). CHD7 also colocalized with NeuroD within the ganglion (Fig. 4D-F), although there a small number of CHD7-positive cells were NeuroD negative (arrow in Fig. 4F). By contrast, most Islet1-positive cells were CHD7 positive, both within the ganglion and also in the ventral otocyst (Fig. 4G-I). The majority of proliferating cells within the ganglion, otocyst and surrounding mesenchyme were also CHD7 positive, based on colocalization of CHD7 with anti-phosphohistone H3 (Fig. 4J-L).

Direct measurement of sectioned tissues showed a 1.5-fold reduction in the size of the E10.5-E12.5 vestibulo-cochlear ganglion between $Chd7^{Gt/+}$ and wild-type embryos (data not shown). β-Tubulin III and Islet1 immunofluorescence were also reduced in $Chd7^{Gt/+}$ and conditional null ganglia compared with wild type (Fig. 5). In $Chd7^{Gt/Gt}$ ganglia, only a small number of cells were β-Tubulin III or Islet1 positive, consistent with severe ganglionic hypoplasia. Quantitation of Islet1-positive cells in the E10.5 vestibulo-cochlear ganglion revealed significantly fewer Islet1-positive cells in $Chd7^{Gt/+}$ (mean=343; s.e.m.=72; n=8) and conditional heterozygous (mean=426; s.e.m.=54; n=8) mice compared with wild type (mean=841; s.e.m.=64; n=8) (Fig. 5I and Table 1). The reduction in Islet1-positive cells was even more severe in $Chd7^{Gt/Gt}$ (mean=14; s.e.m.=4; n=8) and conditional null (mean=130; s.e.m.=18; n=8) embryos (Fig. 5I and Table 1). Reduced *Chd7* mutant ganglia and Islet1-positive neuroblasts together suggest that CHD7 is a positive regulator of inner ear neurogenesis, perhaps via effects on pro-neural gene transcription.

### *Chd7* mutants display defects in primary neurogenesis and ganglionic specification

To address whether reduced expression of pro-neural genes in *Chd7* mutant inner ears reflects a reduction in delaminating neuroblasts, we quantitated the number of NeuroD-positive cells in the E9.5-E11.5 ganglion and otic epithelium (Fig. 6 and Table 2). NeuroD-positive cells in the $Chd7^{Gt/+}$ ventral otic epithelium were significantly reduced at E10.5 (mean=65; s.e.m.=6; n=8) compared with wild-type littermates (mean=91; s.e.m.=7; n=8), but were unchanged at E9.5 and E11.5 (Fig. 6J and Table 2). There were also significantly fewer NeuroD-positive cells in the $Chd7^{Gt/+}$ ganglion at E9.5 (mean=87; s.e.m.=11; n=8) and E10.5 (mean=509; s.e.m.=72; n=8) compared with wild type (E9.5: mean=245; s.e.m.=48; n=8; E10.5: mean=1010; s.e.m.=82; n=8), with no differences observed at E11.5 (see Table 2). Interestingly, NeuroD-positive cells did not accumulate in the $Chd7^{Gt/+}$ epithelium between E9.5-E11.5, suggesting normal delamination from the otocyst. These data suggest a defect in primary neurogenesis in the E10.5 $Chd7^{Gt/+}$ otic epithelium and ganglion, and are consistent with reduced Islet1-positive and TUJ1-positive neuroblasts (Fig. 5). Together, these observations indicate a defect in ganglionic neuronal production or specification. By E11.5, $Chd7^{Gt/+}$ embryos have normal numbers of neuroblasts in the epithelium and ganglion, suggesting that the requirement for CHD7 is temporally restricted to earlier timepoints.

In contrast to $Chd7^{Gt/+}$, analysis of $Chd7^{Gt/Gt}$ embryos showed severe reductions in NeuroD-positive neuroblasts, in both the epithelium and the ganglion at E9.5 and E10.5 (see Fig. 6 and data in Table 2). At E11.5, conditional null embryos also had severe reductions in NeuroD-positive cells in both the epithelium (mean=21; s.e.m.=4; n=8 versus wild type: mean=62; s.e.m.=10; n=8) and ganglion (mean=346; s.e.m.=35; n=8 versus wild type: mean=1082; s.e.m.=66; n=8) (Fig. 6, Table 2). Like $Chd7^{Gt/+}$,
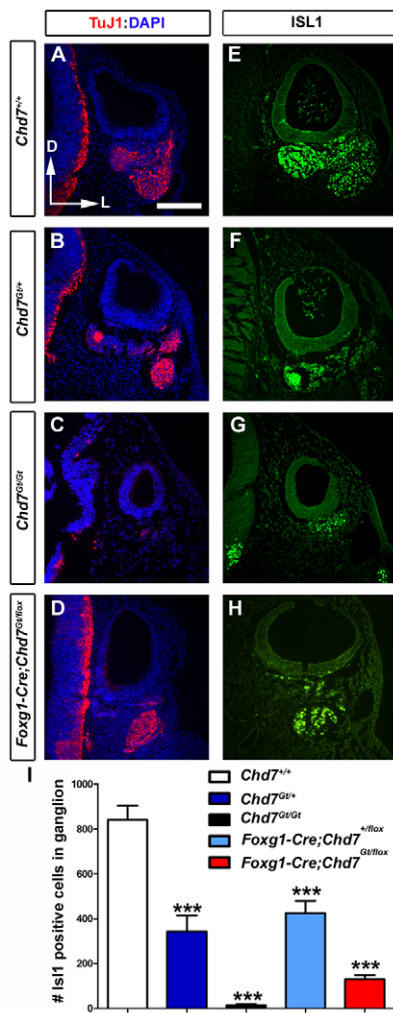
**Fig. 5. *Chd7* germline and conditional mutants have reduced inner ear neuroblasts.** (**A-D**) TuJ1 expression and vestibulo-cochlear ganglia size are reduced in E10.5 *Chd7$^{Gt/+}$* (B), *Chd7$^{Gt/Gt}$* (C) and *Foxg1-Cre;Chd7$^{Gt/flox}$* (D) mutants. (**E-H**) Islet1 positive neuroblasts in the vestibulo-cochlear ganglion are reduced in *Chd7$^{Gt/+}$* (F), *Chd7$^{Gt/Gt}$* (G) and *Foxg1-Cre;Chd7$^{Gt/flox}$* (H) embryos. Sections are in the transverse plane, with dorsal towards the top and lateral towards the right as shown by arrows in A. (**I**) Isl1$^+$ cells are reduced in the ganglion of *Chd7$^{Gt/+}$* (dark blue), *Chd7$^{Gt/Gt}$* (black), *Foxg1-Cre;Chd7$^{+/flox}$* (light blue) and *Foxg-Cre;Chd7$^{Gt/flox}$* (red) as compared with wild type (white). Scale bar: 100 µm. ***$P \leq 0.001$.

conditional heterozygotes also had unchanged NeuroD-positive cells in both the epithelium and ganglion at E11.5 (see Fig. 6, Table 2). Thus, homozygous loss of *Chd7* function, whether in the germline or by *Foxg1-Cre*, results in a more severe defect in inner ear neurogenesis than in *Chd7* heterozygotes and may be related to disruption of the neurogenic domain (Fig. 3BB,GG,DD,JJ).

## CHD7 influences inner ear cell proliferation in a dose- and tissue-dependent manner

Prior studies showed that *Chd7* haploinsufficiency is associated with reduced proliferation of olfactory neural stem cells (Layman et al., 2009). As CHD7 is in proliferating cells of the developing otocyst and stato-acoustic ganglion (Fig. 4J-L), we examined cellular proliferation in E9.5-E10.5 *Chd7* mutant ears using anti-phosphohistone-H3 immunofluorescence (Fig. 7 and Table 3). We observed no change in the number of proliferating cells in the epithelium of *Chd7$^{Gt/+}$* embryos at either E9.5 or E10.5 compared with wild type (Fig. 7 and Table 3). In the *Chd7$^{Gt/+}$* ganglion, cellular proliferation was reduced at E9.5 (mean=7; s.e.m.=2; *n*=8 versus wild type: mean=16; s.e.m.=3; *n*=8) but was unchanged at E10.5 (mean=21; s.e.m.=3; *n*=8 versus wild type: mean=24; s.e.m.=3; *n*=8) (Fig. 7 and Table 3). Likewise, proliferating cells in the E10.5 conditional heterozygous otic epithelium were reduced (mean=53; s.e.m.=4; *n*=8) compared with *Chd7$^{+/flox}$* controls (mean=66; s.e.m.=4; *n*=8), whereas proliferating cells in the ganglion were unchanged (see Fig. 7 and Table 3). We also quantitated mitotic cells within the neurogenic domain, after staining adjacent sections with *Ngn1* and anti-phosphohistone H3 (Fig. 7C-G and see Table S1 in the supplementary material). There were significantly fewer proliferating cells within the neurogenic domain of *Chd7$^{Gt/+}$* ears at E9.5 (mean=23; s.e.m.=3; *n*=8 versus wild type: mean=38; s.e.m.=4; *n*=8) and E10.5 (mean=33; s.e.m.=3; *n*=8 versus wild type: mean=59; s.e.m.=5; *n*=8). Thus, despite normal expression of *Ngn1* in the *Chd7$^{Gt/+}$* neurogenic domain (Fig. 3AA,FF), it contains fewer dividing neuroblasts. This is consistent with fewer migrating neuroblasts (Fig. 5B,F and Fig. 6B,E,H) and a smaller vestibulo-cochlear ganglion.

To test for dose effects, we also examined cellular proliferation in *Chd7$^{Gt/Gt}$* otocysts. *Chd7$^{Gt/Gt}$* embryos had severe reductions in cellular proliferation at E9.5 and E10.5 in both the epithelium and the ganglion (see Fig. 7A,B and Table 3). Analysis of E10.5 conditional null embryos also showed reduced proliferation in both the epithelium (conditional null: mean=34; s.e.m.=2; *n*=8 versus *Chd7$^{+/flox}$* control: mean=66; s.e.m.=4; *n*=8) and ganglion (conditional null: mean=16; s.e.m.=2; *n*=8 versus *Chd7$^{+/flox}$* control: mean=36; s.e.m.=2; *n*=8) (Fig. 7A,B and Table 3). Reduced proliferation in the otic epithelium and ganglion of *Chd7$^{Gt/Gt}$* and *Chd7* conditional null embryos is consistent with significantly reduced or absent expression of neurogenic markers (Fig. 3C,E,R,T,BB,DD), suggesting that *Chd7* has multiple roles that include otic patterning and regulation of proliferation and/or differentiation.

Changes in cell proliferation are often accompanied by alterations in cell death. To test this, we quantified numbers of apoptotic cells in E9.5-E10.5 *Chd7* mutant embryos. We observed no changes in the number of apoptotic cells in E9.5-E10.5 ganglion or otic epithelium of *Chd7$^{Gt/+}$* embryos compared wth wild type (see Fig. S4 and Table S2 in the supplementary material). By contrast, there were significantly fewer apoptotic cells within the *Chd7$^{Gt/Gt}$* ganglion compared with wild type at E9.5 (*Chd7$^{Gt/Gt}$*: mean=8; s.e.m.=3, *n*=8

### Table 1. Quantitation of Islet1-positive cells in the E10.5 ganglion

| Genotype | *Chd7$^{+/+}$* | *Chd7$^{Gt/+}$* | *Chd7$^{Gt/Gt}$* | *Foxg1-Cre;Chd7$^{+/flox}$* | *Foxg1-Cre;Chd7$^{Gt/flox}$* |
|---|---|---|---|---|---|
| Mean | 841 | 343 | 14 | 426 | 130 |
| s.e.m. | 64 | 72 | 4 | 54 | 18 |
| P | – | 0.0002 | <0.0001 | 0.0002 | <0.0001 |
| n (ears) | 8 | 8 | 8 | 8 | 8 |
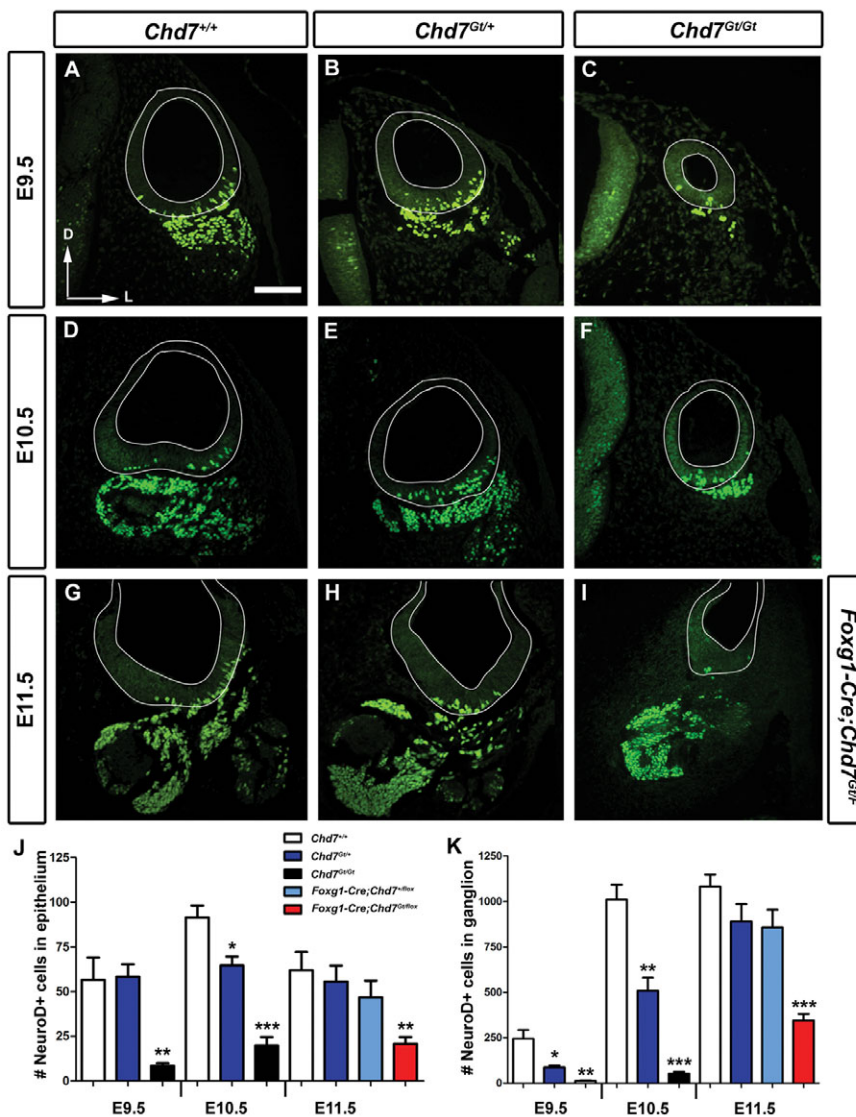
**Fig. 6. Neuroblasts are reduced in both epithelium and ganglion of *Chd7* mutants.** (A-I) Sections are in the transverse plane, with dorsal towards the top and lateral towards the right as shown in A. (A,B,J,K) NeuroD-positive cells are unchanged in the E9.5 *Chd7^{Gt/+}* (B) otic epithelium versus wild-type embryos (A) but decreased in the vestibulo-cochlear ganglion. (A,C,D,F,J,K) NeuroD-positive neuroblasts are significantly reduced in both the epithelium and ganglion of E9.5 and E10.5 *Chd7^{Gt/Gt}* embryos (C,F) relative to wild type (A,D). (D,E,J,K) NeuroD-positive neuroblasts are decreased in both the epithelium and ganglion of E10.5 *Chd7^{Gt/+}* (E) compared with wild type (D). (G-I,J,K) The number of NeuroD-positive cells in the E11.5 epithelium and ganglion is similar in *Chd7^{+/+}* (G), *Chd7^{Gt/+}* (H) and *Foxg1-Cre;Chd7^{+/flox}* (J,K), whereas the number of NeuroD-positive cells in *Foxg1-Cre;Chd7^{Gt/flox}* (I) is significantly decreased. (J,K) *$P \leq 0.05$, **$P \leq 0.005$, ***$P = 0.001$. Scale bar: 100 µm. White lines in A-I delimit the otocyst epithelium.

versus wild type: mean=57; s.e.m.=10, *n*=8) and E10.5 (*Chd7^{Gt/Gt}*: mean=11; s.e.m.=4, *n*=8 versus wild type: mean=41; s.e.m.=8, *n*=8) (see Fig. S4 and Table S2 in the supplementary material). Thus, CHD7 appears to promote early neuroblast proliferation without concomitant increases in cell death.

## DISCUSSION

Here, we describe the first *Chd7^{flox}* allele and its use in inner ear specific loss-of-function studies. We show that *Chd7* conditional null embryos have severe inner ear malformations that affect both vestibular and auditory structures. Complete absence of CHD7 results in decreased expression of patterning and pro-neural (*Otx2*, *Fgf10*, *Ngn1*, *NeuroD* and *Islet1*) genes within the otic epithelium and ganglion (Fig. 8), and reduced proliferation of developing neuroblasts. Our observations support the hypothesis that CHD7 function is essential for proper inner ear morphogenesis and neural development.

### CHD7 is involved in maintenance of *Fgf10*, *Otx2* and *Ngn1* expression

A number of genes involved in inner ear neurogenesis, including *Fgf10*, *Ngn1*, *NeuroD* and *Isl1* are downregulated by *Chd7* deficiency, suggesting that CHD7 is required to maintain

transcription of these genes. NGN1 is crucial for inner ear neurogenesis, as *Ngn1^{-/-}* mice do not display any inner ear sensory neurons (Ma et al., 2000; Ma et al., 1998). NGN1 activates the basic helix-loop-helix protein NeuroD, which is important for neuronal differentiation and survival (Kim et al., 2001). The *Ngn1*-expressing region of the otocyst gives rise to the maculae of the utricle and saccule (Raft et al., 2007). *Ngn1* expression is absent from E9.5-E10.5 *Chd7^{Gt/Gt}* otocysts but is present at low levels in the E9.0 *Chd7^{Gt/Gt}* otocyst and is significantly reduced in E9.5-E10.5 conditional null embryos. This suggests that CHD7 acts upstream of NGN1 within the neurogenesis signaling pathway to maintain *Ngn1* expression, even though it is not required for *Ngn1* induction. Preserved *Ngn1* expression in *Chd7* heterozygous mutant mice (Fig. 3AA) is also consistent with the normal ultrastructure of sensory maculae of the utricle and saccule in these mice (Adams et al., 2007), but does not explain the semicircular canal and other morphogenetic defects.

*Fgf10* expression, which is absent from *Chd7*-null mutant embryos, is required for otic *Ngn1* expression (Alsina et al., 2004). It is conceivable that absence of *Fgf10* expression from *Chd7* conditional null and *Chd7^{Gt/Gt}* otocysts could lead to decreased expression of *Ngn1*. Interestingly, *Fgf10*-null mice have similar

**Table 2. Quantitation of NeuroD-positive cells in the otic epithelium and ganglion**

**A Epithelium**

| Genotype | E9.5 | | | E10.5 | | | E11.5 | | | |
|---|---|---|---|---|---|---|---|---|---|---|
| | $Chd7^{+/+}$ | $Chd7^{Gt/+}$ | $Chd7^{Gt/Gt}$ | $Chd7^{+/+}$ | $Chd7^{Gt/+}$ | $Chd7^{Gt/Gt}$ | $Chd7^{+/+}$ | $Chd7^{Gt/+}$ | $Foxg1\text{-}Cre;Chd7^{+/flox}$ | $Foxg1\text{-}Cre;Chd7^{Gt/flox}$ |
| Mean | 57 | 58 | 9 | 91 | 65 | 20 | 62 | 56 | 47 | 21 |
| s.e.m. | 13 | 7 | 2 | 7 | 6 | 5 | 10 | 9 | 9 | 4 |
| $P$ | – | 0.89986 | 0.0021 | – | 0.0069 | <0.0001 | – | 0.6471 | 0.2901 | 0.0021 |
| $n$ (ears) | 8 | 8 | 8 | 8 | 8 | 8 | 8 | 8 | 8 | 8 |

**B Ganglion**

| Genotype | E9.5 | | | E10.5 | | | E11.5 | | | |
|---|---|---|---|---|---|---|---|---|---|---|
| | $Chd7^{+/+}$ | $Chd7^{Gt/+}$ | $Chd7^{Gt/Gt}$ | $Chd7^{+/+}$ | $Chd7^{Gt/+}$ | $Chd7^{Gt/Gt}$ | $Chd7^{+/+}$ | $Chd7^{Gt/+}$ | $Foxg1\text{-}Cre;Chd7^{+/flox}$ | $Foxg1\text{-}Cre;Chd7^{Gt/flox}$ |
| Mean | 245 | 87 | 13 | 1010 | 509 | 53 | 1082 | 890 | 857 | 346 |
| s.e.m. | 48 | 11 | 4 | 82 | 72 | 11 | 66 | 96 | 97 | 35 |
| $P$ | – | 0.0065 | 0.0003 | – | 0.0004 | <0.0001 | – | 0.1221 | 0.0766 | <0.0001 |
| $n$ (ears) | 8 | 8 | 8 | 8 | 8 | 8 | 8 | 8 | 8 | 8 |

inner ear phenotypes to those in *Chd7* heterozygotes, including defects in innervation to the posterior crista (Adams et al., 2007; Pauley et al., 2003). However, *Chd7*-conditional null ear phenotypes are much more severe, supporting the idea that CHD7 functions upstream of *Fgf10*. *Fgf10* has been shown to enhance the *Foxg1*-null inner ear phenotype (Pauley et al., 2006); however, it is unlikely that the *Chd7* conditional null inner ear defects reported here can be attributed to the presence of *Foxg1-Cre*. *Foxg1*^{+/–} mice are reported to have no inner ear defects, and neurosensory domain specification is unaltered in *Foxg1*^{–/–} mice (Hwang et al., 2009; Pauley et al., 2006).

Interestingly, OTX2 is implicated in mouse cochlear morphogenesis (Morsli et al., 1999). *Otx2* expression is absent from *Chd7*[Gt/Gt] and conditional null otocysts, which may contribute to the cochlear phenotype observed in *Chd7* conditional null embryos. Furthermore, *Otx2* is an important early otic patterning gene and is required for establishment of the

neurogenic domain by repressing *Fgf10* expression (Miyazaki et al., 2006). As both *Otx2* and *Fgf10* expression are absent from *Chd7* null otocysts, CHD7 may regulate *Fgf10* in an OTX2-dependent manner.

## CHD7 acts via *Eya1* and *Lfng* independent pathways, and negatively regulates TBX1

EYA1 is required for formation of the cochlea and vestibulo-cochlear ganglion, and for development of the sensory epithelium (Xu et al., 1999; Zou et al., 2008). *Eya1* expression is absent in *Chd7*[Gt/Gt] embryos, but maintained in conditional null inner ears. Hypomorphic *Eya1* (*Eya1*[bor/bor]) and *Chd7*[Gt/+] embryos show similarly reduced vestibulo-cochlear ganglion size and reductions of NeuroD and Islet1 in delaminating neuroblasts (Friedman et al., 2005). Analysis of *Eya1*-null and hypomorphic alleles showed that EYA1 promotes expression of *Fgf10* and *Otx2* in a dose-dependent manner (Zou et al., 2008). *Otx2* expression is only maintained in
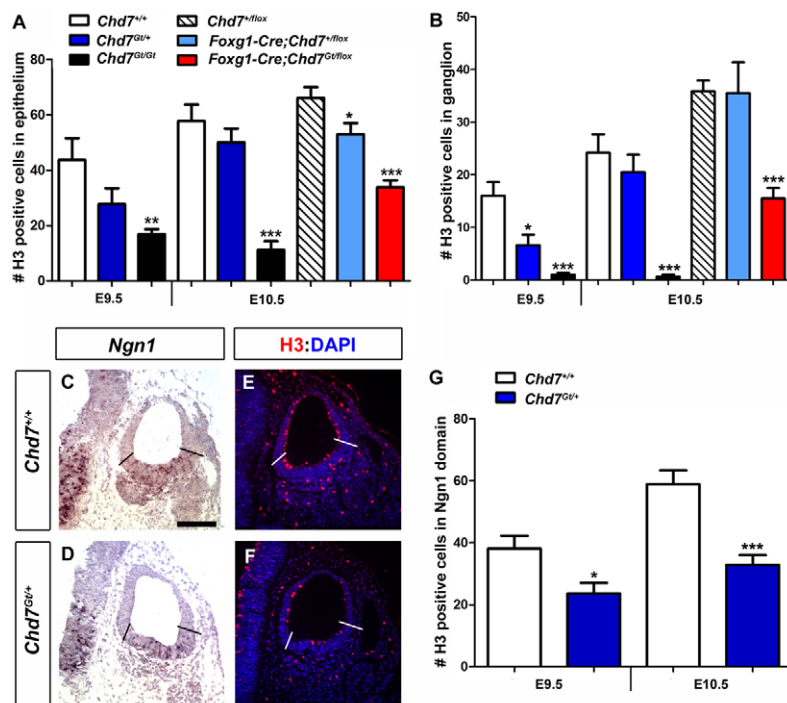


**Fig. 7. CHD7 regulation of inner ear cellular proliferation is dose and tissue dependent.** (**A**,**B**) Significant decreases in numbers of H3-positive cells are noted in the epithelium and ganglion of *Chd7*[Gt/Gt] (black) and *Foxg1-Cre;Chd7*[Gt/flox] (red) embryos compared with controls (white). (**C-F**) Adjacent sections of E10.5 *Chd7*^{+/+} (C,E) and *Chd7*[Gt/+] (D,F) embryos show *Ngn1* mRNA (C,D) and anti-phosphohistone H3 (E,F). Sections are in the transverse plane, with dorsal towards the top and lateral towards the right. Scale bar in C is 100 μm and applies to C-F. (**G**) H3-positive cells are decreased in number in the neurogenic domain of E9.5 and E10.5 *Chd7*[Gt/+] embryos (blue) compared with wild-type littermates (white). *$P \leq 0.01$; **$P \leq 0.005$; ***$P \leq 0.001$.

**Table 3. Quantitation of H3-positive cells in the otic epithelium and ganglion**

**A Epithelium**

| | E9.5 | | | E10.5 | | | | | |
|---|---|---|---|---|---|---|---|---|---|
| Genotype | $Chd7^{+/+}$ | $Chd7^{Gt/+}$ | $Chd7^{Gt/Gt}$ | $Chd7^{+/+}$ | $Chd7^{Gt/+}$ | $Chd7^{Gt/Gt}$ | $Chd7^{+/flox}$ | Foxg1-Cre; $Chd7^{+/flox}$ | Foxg1-Cre; $Chd7^{Gt/flox}$ |
| Mean | 44 | 28 | 17 | 58 | 50 | 11 | 66 | 53 | 34 |
| s.e.m. | 8 | 6 | 2 | 6 | 5 | 3 | 4 | 4 | 2 |
| P | – | 0.1216 | 0.0049 | – | 0.3338 | <0.0001 | – | 0.0353 | <0.0001 |
| n (ears) | 8 | 8 | 8 | 8 | 8 | 8 | 8 | 8 | 8 |

**B Ganglion**

| | E9.5 | | | E10.5 | | | | | |
|---|---|---|---|---|---|---|---|---|---|
| Genotype | $Chd7^{+/+}$ | $Chd7^{Gt/+}$ | $Chd7^{Gt/Gt}$ | $Chd7^{+/+}$ | $Chd7^{Gt/+}$ | $Chd7^{Gt/Gt}$ | $Chd7^{+/flox}$ | Foxg1-Cre; $Chd7^{+/flox}$ | Foxg1-Cre; $Chd7^{Gt/flox}$ |
| Mean | 16 | 7 | 1 | 24 | 21 | 0.6 | 36 | 36 | 16 |
| s.e.m. | 3 | 2 | 0.4 | 3 | 3 | 0.4 | 2 | 6 | 2 |
| P | – | 0.0128 | <0.0001 | – | 0.4517 | <0.0001 | – | 0.9528 | <0.0001 |
| n (ears) | 8 | 8 | 8 | 8 | 8 | 8 | 8 | 8 | 8 |

the ventral otocyst if *Eya1* expression is greater than 25% of normal values (Zou et al., 2008). In heterozygous *Chd7* mutant ears, we observed no changes in expression of *Otx2* or *Fgf10*, whereas *Otx2* and *Fgf10* expression was absent in *Chd7* homozygous null and conditional null ears. $Eya1^{-/-}$ and $Chd7^{Gt/Gt}$ mutants also have expansion of *Tbx1* expression into the ventral region of the otocyst (Fig. 3W) (Friedman et al., 2005). As TBX1 is a suppressor of neural cell fate within the dorsal otocyst (Raft et al., 2004), expansion of *Tbx1* expression into the neurogenic domain could account for the reduced *Ngn1* expression observed in both *Eya1* and *Chd7* mutant mice. It is therefore tempting to attribute the decreased expression of neural-fate markers observed in $Chd7^{Gt/Gt}$ otocysts to absent *Eya1* expression. However, in *Chd7* conditional null otocysts, *Eya1* expression is retained, yet *Otx2* and *Fgf10* expression are absent and *Tbx1* expression is expanded. This suggests that absence of *Eya1* expression within $Chd7^{Gt/Gt}$ embryos is either influenced by tissues other than the otocyst, or is a consequence of the hypoplastic nature of the $Chd7^{Gt/Gt}$ embryo. It also implies that changes in expression of *Otx2, Fgf10* and *Tbx1* in *Chd7* mutant embryos are not regulated through EYA1, but via a parallel molecular genetic pathway (Fig. 8). In addition, $Chd7^{+/-};Tbx1^{+/-}$ double mutants display a more severe inner ear phenotype than do either single heterozygous mutation (Randall et al., 2009), suggesting that CHD7 and TBX1 could regulate the expression of one another. Interestingly, mutations in human *TBX1* contribute to DiGeorge syndrome, a multiple anomaly condition that has phenotypic overlap with CHARGE Syndrome (de Lonlay-Debeney et al., 1997).

*Lfng* expression also correlates with neural fate markers, and defines a ventral region within the otocyst that ultimately gives rise to the saccule and utricle (Morsli et al., 1998). *Lfng* expression is absent from $Eya1^{-/-}$ otocysts and is expanded in $Tbx1^{-/-}$ nulls, consistent with changes in neural fate markers in the otocysts of these mutant mice (Raft et al., 2004; Zou et al., 2008). By contrast, *Lfng* expression is preserved in *Chd7*-null mutants, whereas pro-neural genes are decreased, suggesting that absence of CHD7 specifically affects neuroblast production in the neurogenic domain without completing disrupting patterning of the ventral otocyst. Our data support the hypothesis that CHD7 acts upstream of FGF10 and OTX2, and in parallel with EYA1, to promote inner ear neurogenesis in a dose-dependent manner via inhibition of *Tbx1* and/or activation of the *Ngn1/NeuroD/Isl1* transcriptional regulatory cascade (Fig. 8).

## Dosage effects of CHD7 in neuroblast development

The observed effects of CHD7 deficiency on otocyst gene expression and neuroblast development appear to be highly sensitive to *Chd7* gene dose. Loss of *Chd7* in the germline results in extreme hypoplasia of the embryo and the developing vestibulo-cochlear ganglion, whereas heterozygous loss leads to milder phenotypes. Conditional *Chd7* mutants have intermediate phenotypes, with reduced neuroblast proliferation and pro-neural gene expression. The reasons for these intermediate phenotypes could be related to the timing of onset or tissue specificity of *Cre* expression. There is Cre activity in the developing *Foxg1-Cre* hindbrain (Hebert and McConnell, 2000), and we observed reduced CHD7 in the hindbrain of *Chd7* conditional mutant embryos (Fig. 2C,D). Thus, aberrant signaling from CHD7-dependent pathways in the rhombencephalon could also contribute to the intermediate phenotypes seen in *Foxg1-Cre;Chd7* conditional mutant embryos.

## Evidence for CHD7 as a positive regulator of cell cycle maintenance or progression

Recent observations showed that CHD7 promotes olfactory neural stem cell proliferation (Layman et al., 2009). Here, we demonstrate that heterozygous loss of *Chd7* results in reduced proliferation within the neurogenic domain of the developing otocyst and fewer ganglionic neuroblasts available to proliferate and occupy the developing vestibulo-cochlear ganglion. Conditional *Chd7*-null embryos also have defects in ganglionic and epithelial neuroblast proliferation, in association with a more severe inner ear phenotype. Although CHD7 does not seem to directly regulate apoptosis, the number of apoptotic cells was increased (relative to wild type) in E10.5 mutant ears when normalized to account for the reduced number of NeuroD+ neuroblasts in each region (see Table 2; see Fig. S4 and Table S2 in the supplementary material). Thus, primary reduction of H3+ cells in the neurogenic domain results in fewer neuroblasts available to occupy a smaller mutant ganglion, and this smaller mutant ganglion exhibits relatively increased cell death.

Other members of the CHD protein family have been implicated in proliferation and/or apoptosis (Bagchi et al., 2007; Gaspar-Maia et al., 2009; Nishiyama et al., 2009; Rodriguez-Paredes et al., 2009). In vitro inhibition of *Chd1* creates abnormally high levels of neural differentiation, and is required for maintenance of pluripotency (Gaspar-Maia et al., 2009). CHD8, which has close homology to CHD7, positively controls genes expressed in the G1/S transition phase, and is required for normal proliferation (Rodriguez-Paredes
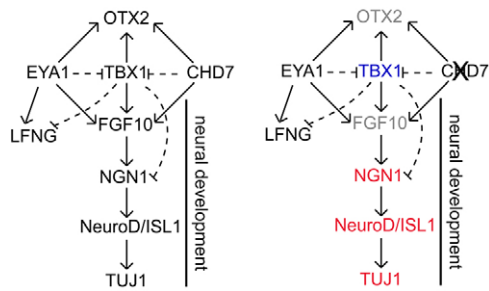
**Fig. 8. Model of CHD7 function in genetic cascades that regulate inner ear neurogenesis based on our expression data and on published reports.** Shown on the left are proposed genetic cascades in wild type, with changes in *Chd7* mutants on the right. Solid and broken lines represent positive and negative regulation of downstream genes, respectively. Genes in grey, red or blue illustrate absent, reduced or increased expression in *Chd7* mutant embryos, respectively. CHD7 activates, either directly or indirectly, expression of FGF10 and NGN1, which results in fewer delaminated NeuroD+, ISL1+ and β-tubulin III (TUJ1)+ neuroblasts. EYA1 also regulates this neurogenic cascade, potentially via CHD7-independent mechanisms. Both CHD7 and EYA1 negatively regulate TBX1, which is an inhibitor of NGN1 and neurogenesis. Like TBX1 and EYA1, CHD7 positively regulates OTX2, which is crucial for cochlear development. LFNG is activated by EYA1 and inhibited by TBX1, but is not sensitive to CHD7 dose.

et al., 2009). In addition, both CHD5 and CHD8 have been implicated as tumor suppressor genes (Bagchi et al., 2007; Nishiyama et al., 2009). Thus, the CHD family of proteins may function as tissue-specific regulators of cell cycle progression. Interestingly, EYA1 is involved in cell cycle maintenance during inner ear neurogenesis. *Eya1*-null embryos display increased apoptosis within the vestibulo-cochlear ganglion and epithelium of the developing ear (Zou et al., 2004; Zou et al., 2006), supporting the hypothesis that CHD7 and EYA1 could act in parallel pathways by complementary regulation of cell cycle progression.

## Downstream genetic targets of CHD7

In *Drosophila*, the CHD7 ortholog *kismet* regulates transcriptional elongation via occupancy at sites of active transcription and RNA polymerase II binding (Srinivasan et al., 2005; Srinivasan et al., 2008). Kismet is required for transcription of the pro-neural factor *atonal* (*Atoh1*) and regulation of retinal photoreceptor cell development (Melicharek et al., 2008). CHD family members also play important roles in proliferation and/or apoptosis, raising the possibility that chromatin regulation of mitosis and programmed cell death may be widespread during development. The global hypoplasia observed in *Chd7*^Gt/Gt^ embryos, combined with in vitro evidence that CHD7 binds a large number of target genes (Schnetz et al., 2009), also suggests that CHD7 may positively regulate proliferation in many tissues. Thus, germline loss of *Chd7* may not accurately reflect the tissue-specific roles of CHD7 in gene regulation, highlighting the importance of examining conditional loss of *Chd7* in vivo.

Using our newly generated *Chd7*^flox^ allele, we showed that CHD7 deficiency activates or represses expression of a number of genes essential for inner ear neurogenesis in a dose-dependent manner. It is not known whether CHD7 acts directly or indirectly, alone or in combination with other co-factors to alter transcription of inner ear neural-fate genes. ChIP-chip data in pluripotent cell lines suggest that

CHD7 deficiency leads to many changes in gene expression of small effect sizes (Schnetz et al., 2009). By contrast, our results show that CHD7 can exert large effects on transcription of a small number of crucial genes during development. The tissue-specific phenotypes that result from CHD7 deficiency could be related to changes in these crucial developmental regulator genes. Future studies will help determine whether CHD7 functions differently in multipotent versus differentiated cells, and whether its ability to promote proliferation and neurogenesis involves distinct molecular mechanisms or co-factors.

In summary, our data provide a basis for understanding how chromatin regulatory proteins influence the proliferative potential of inner ear progenitors during development. Still, unresolved issues remain. It is not known whether overexpression of *Ngn1* or other pro-neural genes rescues *Chd7* mutant phenotypes, or whether CHD7 exerts its effects via changes in transcriptional initiation or elongation. The composition of CHD7-containing complexes that mediate CHD7 effects in neural tissues is also not known, and it will be interesting to see whether this complex changes as progenitors switch to the postmitotic state. There is evidence for chromatin protein subunit switching during neurogenesis (Lessard et al., 2007; Yoo and Crabtree, 2009; Yoo et al., 2009), and further studies will determine whether similar or related mechanisms occur in developing inner ear neuroblasts.

### Competing interests statement
The authors declare no competing financial interests.

### Supplementary material
Supplementary material for this article is available at
http://dev.biologists.org/lookup/suppl/doi:10.1242/dev.047894/-/DC1

### References
**Adams, M. E., Hurd, E. A., Beyer, L. A., Swiderski, D. L., Raphael, Y. and Martin, D. M.** (2007). Defects in vestibular sensory epithelia and innervation in mice with loss of Chd7 function: implications for human CHARGE syndrome. *J. Comp. Neurol.* **504**, 519-532.

**Alsina, B., Abello, G., Ulloa, E., Henrique, D., Pujades, C. and Giraldez, F.** (2004). FGF signaling is required for determination of otic neuroblasts in the chick embryo. *Dev. Biol.* **267**, 119-134.

**Alsina, B., Giraldez, F. and Pujades, C.** (2009). Patterning and cell fate in ear development. *Int. J. Dev. Biol.* **53**, 1503-1513.

**Bagchi, A., Papazoglu, C., Wu, Y., Capurso, D., Brodt, M., Francis, D., Bredel, M., Vogel, H. and Mills, A. A.** (2007). CHD5 is a tumor suppressor at human 1p36. *Cell* **128**, 459-475.

**Bajpai, R., Chen, D. A., Rada-Iglesias, A., Zhang, J., Xiong, Y., Helms, J., Chang, C. P., Zhao, Y., Swigut, T. and Wysocka, J.** (2010). CHD7 cooperates with PBAF to control multipotent neural crest formation. *Nature* **463**, 958-962.

**Bok, J., Chang, W. and Wu, D. K.** (2007). Patterning and morphogenesis of the vertebrate inner ear. *Int. J. Dev. Biol.* **51**, 521-533.

**Bosman, E. A., Penn, A. C., Ambrose, J. C., Kettleborough, R., Stemple, D. L. and Steel, K. P.** (2005). Multiple mutations in mouse Chd7 provide models for CHARGE syndrome. *Hum. Mol. Genet.* **14**, 3463-3476.

**de Lonlay-Debeney, P., Cormier-Daire, V., Amiel, J., Abadie, V., Odent, S., Paupe, A., Couderc, S., Tellier, A. L., Bonnet, D., Prieur, M. et al.** (1997). Features of DiGeorge syndrome and CHARGE association in five patients. *J. Med. Genet.* **34**, 986-989.

**Fekete, D. M. and Wu, D. K.** (2002). Revisiting cell fate specification in the inner ear. *Curr. Opin. Neurobiol.* **12**, 35-42.

**Friedman, R. A., Makmura, L., Biesiada, E., Wang, X. and Keithley, E. M.** (2005). Eya1 acts upstream of Tbx1, Neurogenin 1, NeuroD and the neurotrophins BDNF and NT-3 during inner ear development. *Mech. Dev.* **122**, 625-634.

Fritzsch, B., Pirvola, U. and Ylikoski, J. (1999). Making and breaking the innervation of the ear: neurotrophic support during ear development and its clinical implications. *Cell Tissue Res.* **295**, 369-382.

Fritzsch, B., Pauley, S., Matei, V., Katz, D. M., Xiang, M. and Tessarollo, L. (2005). Mutant mice reveal the molecular and cellular basis for specific sensory connections to inner ear epithelia and primary nuclei of the brain. *Hear Res.* **206**, 52-63.

Fritzsch, B., Beisel, K. W. and Hansen, L. A. (2006). The molecular basis of neurosensory cell formation in ear development: a blueprint for hair cell and sensory neuron regeneration? *BioEssays* **28**, 1181-1193.

Gaspar-Maia, A., Alajem, A., Polesso, F., Sridharan, R., Mason, M. J., Heidersbach, A., Ramalho-Santos, J., McManus, M. T., Plath, K., Meshorer, E. et al. (2009). Chd1 regulates open chromatin and pluripotency of embryonic stem cells. *Nature* **460**, 863-868.

Hebert, J. M. and McConnell, S. K. (2000). Targeting of cre to the Foxg1 (BF-1) locus mediates loxP recombination in the telencephalon and other developing head structures. *Dev. Biol.* **222**, 296-306.

Hurd, E. A., Capers, P. L., Blauwkamp, M. N., Adams, M. E., Raphael, Y., Poucher, H. K. and Martin, D. M. (2007). Loss of Chd7 function in gene-trapped reporter mice is embryonic lethal and associated with severe defects in multiple developing tissues. *Mamm. Genome* **18**, 94-104.

Hwang, C. H., Simeone, A., Lai, E. and Wu, D. K. (2009). Foxg1 is required for proper separation and formation of sensory cristae during inner ear development. *Dev. Dyn.* **238**, 2725-2734.

Kim, W. Y., Fritzsch, B., Serls, A., Bakel, L. A., Huang, E. J., Reichardt, L. F., Barth, D. S. and Lee, J. E. (2001). NeuroD-null mice are deaf due to a severe loss of the inner ear sensory neurons during development. *Development* **128**, 417-426.

Layman, W. S., McEwen, D. P., Beyer, L. A., Lalani, S. R., Fernbach, S. D., Oh, E., Swaroop, A., Hegg, C. C., Raphael, Y., Martens, J. R. et al. (2009). Defects in neural stem cell proliferation and olfaction in Chd7 deficient mice indicate a mechanism for hyposmia in human CHARGE syndrome. *Hum. Mol. Genet.* **18**, 1909-1923.

Lessard, J., Wu, J. I., Ranish, J. A., Wan, M., Winslow, M. M., Staahl, B. T., Wu, H., Aebersold, R., Graef, I. A. and Crabtree, G. R. (2007). An essential switch in subunit composition of a chromatin remodeling complex during neural development. *Neuron* **55**, 201-215.

Ma, Q., Chen, Z., del Barco Barrantes, I., de la Pompa, J. L. and Anderson, D. J. (1998). neurogenin1 is essential for the determination of neuronal precursors for proximal cranial sensory ganglia. *Neuron* **20**, 469-482.

Ma, Q., Anderson, D. J. and Fritzsch, B. (2000). Neurogenin 1 null mutant ears develop fewer, morphologically normal hair cells in smaller sensory epithelia devoid of innervation. *J. Assoc. Res. Otolaryngol.* **1**, 129-143.

Martin, D. M., Skidmore, J. M., Fox, S. E., Gage, P. J. and Camper, S. A. (2002). Pitx2 distinguishes subtypes of terminally differentiated neurons in the developing mouse neuroepithelium. *Dev. Biol.* **252**, 84-99.

Martin, D. M., Skidmore, J. M., Philips, S. T., Vieria, C., Gage, P. J., Condie, B. G., Raphael, Y., Martinez, S. and Camper, S. A. (2004). PITX2 is required for normal development of neurons in the mouse subthalamic nucleus and midbrain. *Dev. Biol.* **267**, 93-108.

Melicharek, D., Shah, A., DiStefano, G., Gangemi, A. J., Orapallo, A., Vrailas-Mortimer, A. D. and Marenda, D. R. (2008). Identification of novel regulators of atonal expression in the developing Drosophila retina. *Genetics* **180**, 2095-2110.

Miyazaki, H., Kobayashi, T., Nakamura, H. and Funahashi, J. (2006). Role of Gbx2 and Otx2 in the formation of cochlear ganglion and endolymphatic duct. *Dev. Growth Differ.* **48**, 429-438.

Morsli, H., Choo, D., Ryan, A., Johnson, R. and Wu, D. K. (1998). Development of the mouse inner ear and origin of its sensory organs. *J. Neurosci.* **18**, 3327-3335.

Morsli, H., Tuorto, F., Choo, D., Postiglione, M. P., Simeone, A. and Wu, D. K. (1999). Otx1 and Otx2 activities are required for the normal development of the mouse inner ear. *Development* **126**, 2335-2343.

Nioi, P., Nguyen, T., Sherratt, P. J. and Pickett, C. B. (2005). The carboxy-terminal Neh3 domain of Nrf2 is required for transcriptional activation. *Mol. Cell. Biol.* **25**, 10895-10906.

Nishiyama, M., Oshikawa, K., Tsukada, Y., Nakagawa, T., Iemura, S., Natsume, T., Fan, Y., Kikuchi, A., Skoultchi, A. I. and Nakayama, K. I. (2009). CHD8 suppresses p53-mediated apoptosis through histone H1 recruitment during early embryogenesis. *Nat. Cell Biol.* **11**, 172-182.

Pauley, S., Wright, T. J., Pirvola, U., Ornitz, D., Beisel, K. and Fritzsch, B. (2003). Expression and function of FGF10 in mammalian inner ear development. *Dev. Dyn.* **227**, 203-215.

Pauley, S., Lai, E. and Fritzsch, B. (2006). Foxg1 is required for morphogenesis and histogenesis of the mammalian inner ear. *Dev. Dyn.* **235**, 2470-2482.

Pirvola, U. and Ylikoski, J. (2003). Neurotrophic factors during inner ear development. *Curr. Top. Dev. Biol.* **57**, 207-223.

Raft, S., Nowotschin, S., Liao, J. and Morrow, B. E. (2004). Suppression of neural fate and control of inner ear morphogenesis by Tbx1. *Development* **131**, 1801-1812.

Raft, S., Koundakjian, E. J., Quinones, H., Jayasena, C. S., Goodrich, L. V., Johnson, J. E., Segil, N. and Groves, A. K. (2007). Cross-regulation of Ngn1 and Math1 coordinates the production of neurons and sensory hair cells during inner ear development. *Development* **134**, 4405-4415.

Randall, V., McCue, K., Roberts, C., Kyriakopoulou, V., Beddow, S., Barrett, A. N., Vitelli, F., Prescott, K., Shaw-Smith, C., Devriendt, K. et al. (2009). Great vessel development requires biallelic expression of Chd7 and Tbx1 in pharyngeal ectoderm in mice. *J. Clin. Invest.* **119**, 3301-3310.

Riccomagno, M. M., Martinu, L., Mulheisen, M., Wu, D. K. and Epstein, D. J. (2002). Specification of the mammalian cochlea is dependent on Sonic hedgehog. *Genes Dev.* **16**, 2365-2378.

Riccomagno, M. M., Takada, S. and Epstein, D. J. (2005). Wnt-dependent regulation of inner ear morphogenesis is balanced by the opposing and supporting roles of Shh. *Genes Dev.* **19**, 1612-1623.

Rodriguez-Paredes, M., Ceballos-Chavez, M., Esteller, M., Garcia-Dominguez, M. and Reyes, J. C. (2009). The chromatin remodeling factor CHD8 interacts with elongating RNA polymerase II and controls expression of the cyclin E2 gene. *Nucleic Acids Res.* **37**, 2449-2460.

Sanchez-Calderon, H., Milo, M., Leon, Y. and Varela-Nieto, I. (2007). A network of growth and transcription factors controls neuronal differentation and survival in the developing ear. *Int. J. Dev. Biol.* **51**, 557-570.

Schnetz, M. P., Bartels, C. F., Shastri, K., Balasubramanian, D., Zentner, G. E., Balaji, R., Zhang, X., Song, L., Wang, Z., Laframboise, T. et al. (2009). Genomic distribution of CHD7 on chromatin tracks H3K4 methylation patterns. *Genome Res.* **19**, 590-601.

Srinivasan, S., Armstrong, J. A., Deuring, R., Dahlsveen, I. K., McNeill, H. and Tamkun, J. W. (2005). The Drosophila trithorax group protein Kismet facilitates an early step in transcriptional elongation by RNA Polymerase II. *Development* **132**, 1623-1635.

Srinivasan, S., Dorighi, K. M. and Tamkun, J. W. (2008). Drosophila Kismet regulates histone H3 lysine 27 methylation and early elongation by RNA polymerase II. *PLoS Genet.* **4**, e1000217.

Tai, H. H., Geisterfer, M., Bell, J. C., Moniwa, M., Davie, J. R., Boucher, L. and McBurney, M. W. (2003). CHD1 associates with NCoR and histone deacetylase as well as with RNA splicing proteins. *Biochem. Biophys. Res. Commun.* **308**, 170-176.

Takada, I., Mihara, M., Suzawa, M., Ohtake, F., Kobayashi, S., Igarashi, M., Youn, M. Y., Takeyama, K., Nakamura, T., Mezaki, Y. et al. (2007). A histone lysine methyltransferase activated by non-canonical Wnt signalling suppresses PPAR-gamma transactivation. *Nat. Cell Biol.* **9**, 1273-1285.

Tong, J. K., Hassig, C. A., Schnitzler, G. R., Kingston, R. E. and Schreiber, S. L. (1998). Chromatin deacetylation by an ATP-dependent nucleosome remodelling complex. *Nature* **395**, 917-921.

Vertegaal, A. C., Andersen, J. S., Ogg, S. C., Hay, R. T., Mann, M. and Lamond, A. I. (2006). Distinct and overlapping sets of SUMO-1 and SUMO-2 target proteins revealed by quantitative proteomics. *Mol. Cell. Proteomics* **5**, 2298-2310.

Vissers, L. E., van Ravenswaaij, C. M., Admiraal, R., Hurst, J. A., de Vries, B. B., Janssen, I. M., van der Vliet, W. A., Huys, E. H., de Jong, P. J., Hamel, B. C. et al. (2004). Mutations in a new member of the chromodomain gene family cause CHARGE syndrome. *Nat. Genet.* **36**, 955-957.

Woodage, T., Basrai, M. A., Baxevanis, A. D., Hieter, P. and Collins, F. S. (1997). Characterization of the CHD family of proteins. *Proc. Natl. Acad. Sci. USA* **94**, 11472-11477.

Xu, P. X., Adams, J., Peters, H., Brown, M. C., Heaney, S. and Maas, R. (1999). Eya1-deficient mice lack ears and kidneys and show abnormal apoptosis of organ primordia. *Nat. Genet.* **23**, 113-117.

Yoo, A. S. and Crabtree, G. R. (2009). ATP-dependent chromatin remodeling in neural development. *Curr. Opin. Neurobiol.* **19**, 120-126.

Yoo, A. S., Staahl, B. T., Chen, L. and Crabtree, G. R. (2009). MicroRNA-mediated switching of chromatin-remodelling complexes in neural development. *Nature* **460**, 642-646.

Zou, D., Silvius, D., Fritzsch, B. and Xu, P. X. (2004). Eya1 and Six1 are essential for early steps of sensory neurogenesis in mammalian cranial placodes. *Development* **131**, 5561-5572.

Zou, D., Silvius, D., Rodrigo-Blomqvist, S., Enerback, S. and Xu, P. X. (2006). Eya1 regulates the growth of otic epithelium and interacts with Pax2 during the development of all sensory areas in the inner ear. *Dev. Biol.* **298**, 430-441.

Zou, D., Erickson, C., Kim, E. H., Jin, D., Fritzsch, B. and Xu, P. X. (2008). Eya1 gene dosage critically affects the development of sensory epithelia in the mammalian inner ear. *Hum. Mol. Genet.* **17**, 3340-3356.